Characterization of Metal Doped Carbons by Mercury Porosimetry

M. AFZAL, F. MAHMOOD AND M. SALEEM
Department of Chemistry, Quaid-i-Azam University, Islamabad, Pakistan

(Received 26th September, 1992, revised 30th January, 1993)

Summary: Surface areas and pore structure studies were carried out for metal doped carbons (Ni, Cu, Cd and Zn) containing different fraction of metals. It is observed that mercury intrusion and extrusion curves are irreversible giving the evidence of "ink bottle" pores in the carbon samples. Results indicate that the surface areas obtained by mercury porosimetry are very small comparative to the surface areas determined by nitrogen adsorption. Low values of surface areas by mercury porosimetry indicate the presence of a microporous system which is only accessible to nitrogen molecules but not to mercury.

Introduction

A well known method of determining the pore size distribution is by the analysis of gas adsorption isotherms in the range where capillary condensation accompanies physical adsorption. The method originated by Barrett *et al.*, [1] covered a limited range of pore aradii from 15 Å up to about 200 Å, so that for the study of the distribution above this upper limit other methods had to be found. Washburn and co-workers were the first who suggest the utilization of the phenomenon of capillary depression for this purpose [2,3]. In this method, an adsorbent is immersed into a non-wetting liquid and the liquid is penetrated into its pores by the action of external pressure. Ritter and Drake [4] were first who put Washburn's conception to the practical use, using mercury as a penetrating liquid at pressure up to 1000 atmpsphere. They developed one of the earliest high pressure porosimeters and measured the contact angle between mercury and variety of materials.

Results and Discussion

The plots of intrusion volume, V_{int} versus applied pressure P for active carbon and copper doped carbon ($Cu_{0.0158}$ - C) are given in (Figs. 1 and 2). These plots show that there is a steep initial portion in the intrusion plot which gradually go down at higher pressure. Thereafter, as the applied pressure further increases, there is again relatively sharp increase in the intrusion of mercury. The initial step slope of the intrusion plot may be considered to be a consequence of penetration of mercury into the interparticulate spaces [5]. Once mercury has gained entry into the interparticulate spaces, the slope of the plot flattens. As the pressure further increases, mercury is forced into the pores of carbon having the restricted openings. The extrusion curves show that mercury extrusion do not follow the same path and after a small decrease in intruded volume at high pressure, no further mercury extrusion was observed. It is observed that after penetration and retraction approximately 80% of the mercury remained in the pores of carbon samples. The irreversibility of the hysteresis indicates that the pores of active carbon are not cylindrical in nature. It is believed that if a sample having only cylindrical pores with constant cross section, and providing the advancing and receding contact angles are equal, the point of penetration and retraction of mercury will fall on the same line. Emmett [6] reported that the mercury is not completely removed from the pores because the pore system deviate from the simple picture of cylindrical pores. According to Zhdanov [7] the fraction of mercury retained in the pores may amount 27 to 95% depending on the pore structure of the active carbon. The most extensive study of hysteresis in high pressure porosimetry was made by Kamakin [8], who used an alumina-silica sample. Kamakin believes that irreversibility of hysteresis is due to the fact that (for instance a very long equilibration time) mercury cannot be reversibly retracted from pores with a minimum opening $r \backsim 75$ Å. It is also observed that the samples showing the lower mercury hysteresis are those that exhibit little or no water hysteresis [9]. The irreversibility of hysteresis shows the evidence of "ink bottle" pores in the carbon samples

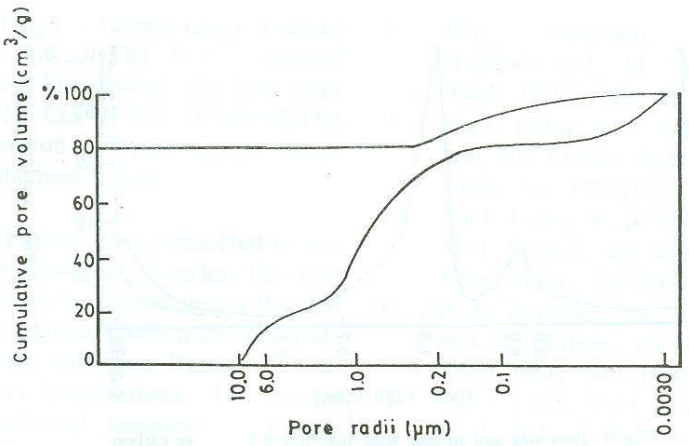

Fig. 1: Mercury intrusion and extrusion curves for active carbon.

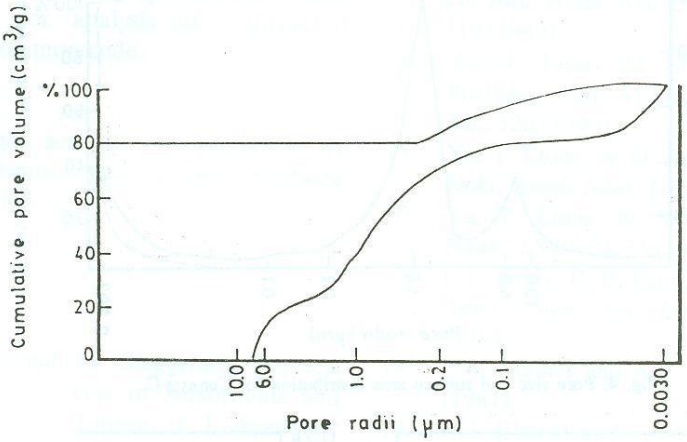

Fig. 2: Mercury intrusion and extrusion curves for $Cu_{0.0535}$-C

that are wider in the interior that at the exit, so that mercury cannot enter until the pressure has risen to the value corresponding to the radius of the entrance capillary. Once this pressure is realized, however, the entire space fills, thus giving an erroneously high apparent pore volume of capillaries of that size. Such a situation lead to a hysteresis effect, i.e. on reducing the pressure, mercury do not leave the entrance capillary at the appropriate pressure due to the presence of ink bottle pores. Evidences for this explanation has also been obtained by observing the structure of the active carbon with the electron microscope [10].

For metal doped carbons, same behaviour in hysteresis is also observed except that the volume of intruded mercury is relatively low than that of the parent active carbon.

The results of pore size distribution in which volume of mercury is transferred to pores as the function of effective radii r are given in Figs. (3 and 4). Pore size distribution curve for active carbon indicates three maxima occurring at effective pore radius of 7.0, 1.43 and 0.0030 μm. The first peak is due to the penetration of mercury in the interparticle spaces. The height of other two peaks shows that the contribution of pores of radius 1.43 μm is more significant to the total pore volume. For copper doped carbon, these maxima occurred nearly at the same pore radius but the volume of intruded mercury is relatively low than that of the active carbon. The effect of metal doping on the meso and macroporosity of active carbon is shown in histograms (Figs. 5-8). The analysis of these histograms gives an idea about the effect of metal doping on the meso and macroporosity .of active

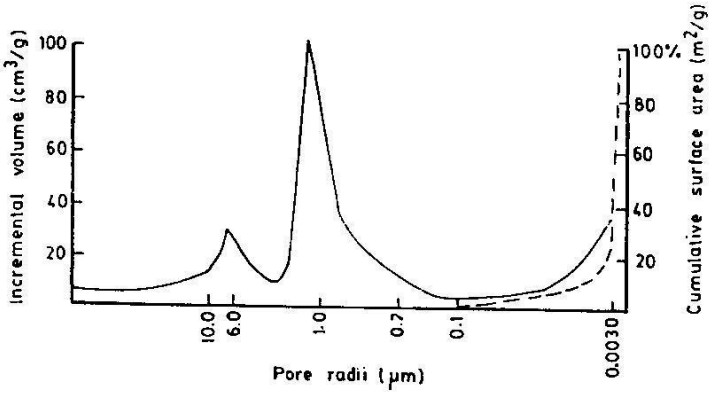

Fig. 3: Pore size and surface area distribution for active carbon.

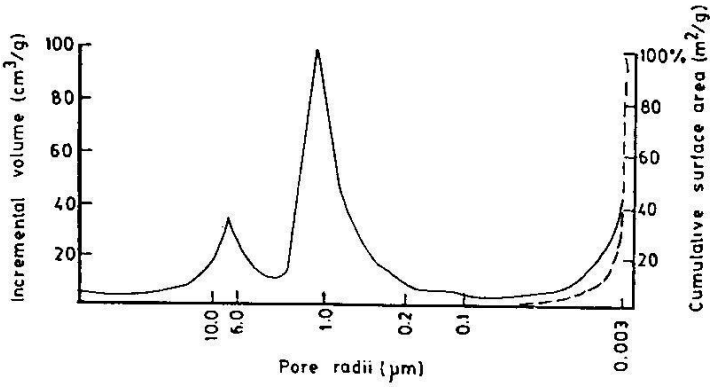

Fig. 4: Pore size and surface area distribution for $Cu_{0.0535}$-C.

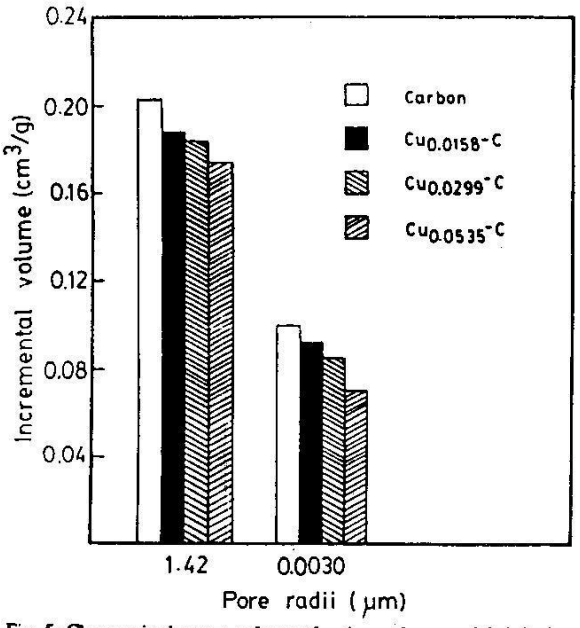

Fig. 5: Changes in the pore volume of active carbon on nickel doping.

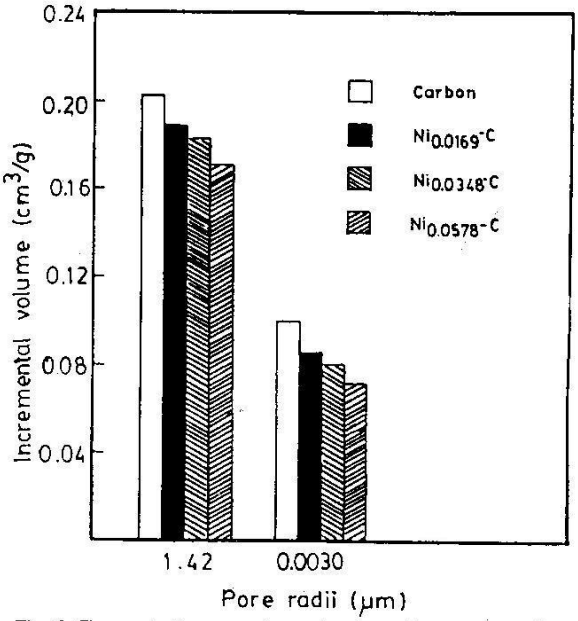

Fig. 6: Changes in the pore volume of active carbon on copper doping.

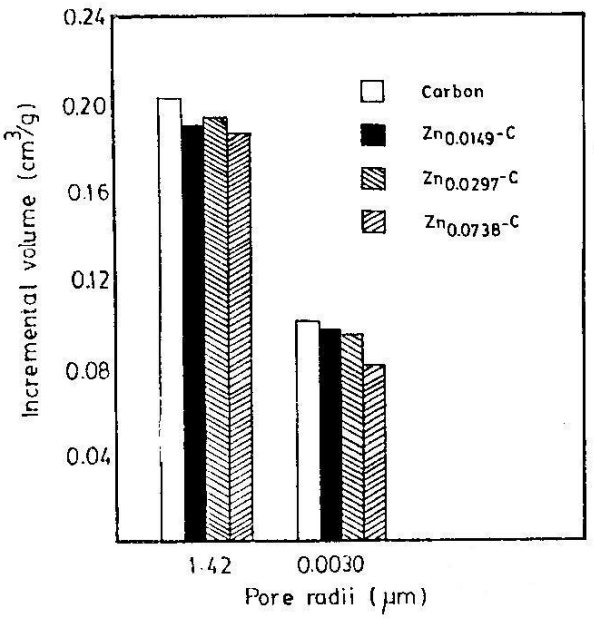

Fig. 7: Changes in the pore volume of active carbon on zinc doping.

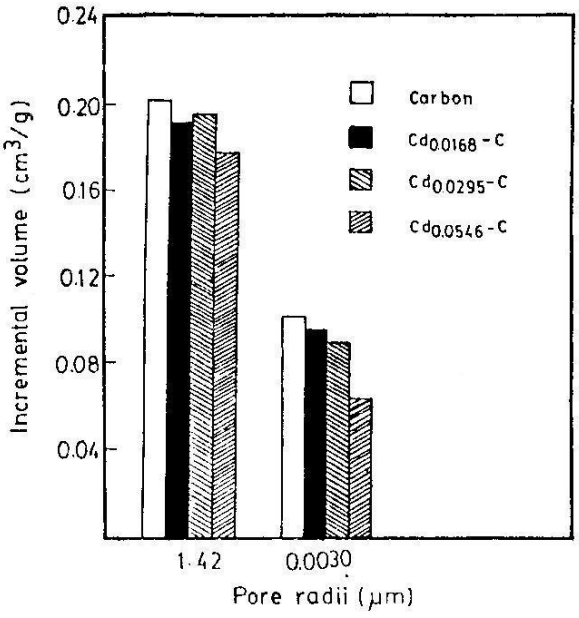

Fig. 8: Changes in the pore volume of active carbon on cadmium doping.

carbon. It can be observed that mesopore volume of active carbon decrease with the increasing amount of doped metal in the carbon lattice. At low metal concentration, the effect is negligible but at high metal loading, there is a considerable decrease in mesoporosity of active carbon and a maximum decrease of 17% was observed for cadmium doped carbon.

By comparing the results for pore volume obtained by the porosimetry and nitrogen adsorption, it is noted that the volume of macro and mesopores given by porosimetric measurements are considerably higher as observed by many other workers [11,12]. They explained that in active carbons there are a considerable number of macropores with entrance openings of sizes which are typical for the size range of transitional pores. These macropores are filled with mercury under the pressure sufficient for its penetration for mesopore entrance. As a result of this the distribution curve obtained does not describe the distribution of pore volumes according to their effective radii but according to radii of the largest of the entrance necks. It means that for active carbon in which measopores with constricted necks are present, only adsorption data provide correct information on the volume and the distribution of transitional pores. However, for active carbon in which pore different from the ink bottle shape are present, good agreement between the structural and distribution curves was obtained [13-16].

The surface areas of carbon samples determined by means of mercury penetration are given in Tables 1-4. It can been seen that these surface areas do not coincide with the surface area found from nitrogen adsorption. For example, the surface area of active carbon was found to be 197 m^2/g by mercury penetration method. However, from nitrogen adsorption isotherm, much higher surface area, *viz* 849 m^2/g for active carbon was deduced. Small surface area by mercury porosimetry indicates the presence of a microporous system which is only accessible to nitrogen molecules but not to mercury. It means that higher value of surfae area by nitrogen adsorption is totally attributable to microporosity of active carbon which cannot be determined by mercury porosimetric method.

Experimental

Active carbon was supplied by Merck (catalog No. 2184). It was washed several times by

Table 1: Mercury porosity data for nickel doped carbons

S. No.	Sample	Total intrusion volume (cm^3/g)	Surface area (m^2/g)	Average pore diameter (nm)	BET surface area (m^2/g)
1.	Carbon	1.2306	197	2.499	849
2.	$Ni_{0.0169}$-C	1.1891	184	2.585	801
3.	$Ni_{0.0348}$-C	1.1601	175	2.652	793
4.	$Ni_{0.0578}$-C	1.1280	169	2.669	771
5.	$Ni_{0.0728}$-C	1.0813	158	2.737	754
6.	$Ni_{0.0931}$-C	1.0632	148	2.874	731

Table 2: Mercury porosity data for copper doped carbons

S. No.	Sample	Total intrusion volume (cm^3/g)	Surface area (m^2/g)	Average pore diameter (nm)	BET surface area (m^2/g)
1.	$Cu_{0.0158}$-C	1.9133	176	2.759	791
2.	$Cu_{0.0299}$-C	1.886	180	2.625	782
3.	$Cu_{0.0535}$-C	1.1666	168	2.777	760
4.	$Cu_{0.0775}$-C	1.1318	170	2.663	753
5.	$Cu_{0.0904}$-C	1.0816	162	2.671	736

Table 3: Mercury porosity data for zinc doped carbons

S. No.	Sample	Total intrusion volume (cm^3/g)	Surface area (m^2/g)	Average pore diameter (nm)	BET surface area (m^2/g)
1.	$Zn_{0.0297}$-C	1.1933	184	2.594	799
2.	$Zn_{0.0532}$-C	1.1313	173	2.615	786
3.	$Zn_{0.0748}$-C	1.0822	161	2.689	763
4.	$Zn_{0.0922}$-C	1.0113	149	2.720	746

Table 4: Mercury porosity data for cadmium doped carbons.

S. No.	Sample	Total intrusion volume (cm^3/g)	Surface area (m^2/g)	Average pore diameter (nm)	BET surface area (m^2/g)
1.	$Cd_{0.0295}$-C	1.1213	173	2.593	754
2.	$Cd_{0.0356}$-C	1.0913	159	2.745	738
3.	$Cd_{0.0546}$-C	1.0553	152	2.777	709
4.	$Cd_{0.0750}$-C	0.9263	139	2.887	675

immersion in distilled water until there was no change in the pH. The divalent metal chlorides used were supplied by Merck with purities better than 99%.

For doping of active carbon, a predetermined amount of metal chloride was magnetically stirred in 200 ml of distilled water and 10 g of active carbon was added to the mixture. The mixture was stirred for 8 h at 373° K until a slurry was formed which was then dried under vacuum at 353° K for 3 h. The dried samples were than heated at 735° K for 5h under the nitrogen atmosphere. A blank carbon samples was also prepared using the same treatment except that distilled water was used in place of metal chloride solution.

For measurement of metal concentration 1 g of the sample was thoroughly stirred with 0.1 N perchloric acid for 4 h at room temperature. The total amount of the metal in solution was then determined by atomic absorption spectrophotometry (Zeiss, Model FMD 47).

The metal doped carbon samples are designated by the following formula M_x-C, where M stands for Ni, Cu, Zn and Cd and x represents in the number of moles of metal per 100 g of carbon.

Before mercury porosimetric measurement, carbon samples were dehydrated by keeping at 60°C overnight in a vacuum oven. A sample of 0.1 - 0.3 g of dried sample was used for porosity measurement. The instrument used was Mercury porosimeter, Autopore II 3220 form micromeritics, mercury surface tension 485.0 dyne/cm and contact angle 130 deg. were used.

All the data was corrected for compression of mercury by taking blank measurement with mercury.

References

1. E. P. Barrett, L. G. Joyner and P. P. Halenda, *J. Am. Chem. Soc.*, 73, 373 (1951).
2. E. W. Washburn, *Proc. Nat. Acad. Sci.*, 7, 115 (1921).
3. E. W. Washburn and E. W. Bunting, *J. Am. Ceram.*, 5, 48 (1922).
4. H. L. Ritter and L. C. Drake, *Ind. Eng. Chem. Anal. Ed.*, 17, 782 (1945).
5. C. H. Giles, D. C. Havard, W. McMillan, T. Smith and R. Wilson, in Characterisation of Porous, Proc. Sym. Ed., S.J. Gregg, K. S.W. Sing and H. F. Stoeckli, Soc. Chem. Ind., London, 267 (1979).
6. P. H. Emmett, *Chem. Rev.*, 43, 69 (1948).
7. S. P. Zhdanov, "Methods of study of the structure of highly dispersed and porous

materials - Papers of the 2nd conference) Editor M. M. Dubinin, *Izd. Aka. Nauk. Mascow*, 251 (1958).

8. N. N. Kamakin, "Methoden der Strukturuntersuchung an Hoechdispersen und porosen Stoffen" (Translated from a Russian edition by Witzmann, H.) Akademie-Verlag, Berling, p. 73.
9. R. M. Barrer, N. McKenzie and J. S. S. Reay, *J. Colloid Sci.*, **11**, 479 (1956).
10. M. M. Dubinin, M. M. Vishnyakova, E. A. Leontev, V. M. Lukyanovich and A. I. Sarachov, *Zhur. fiz. khim.*, **34**, 2019 (1980).
11. P. L. Walker Jr., F. Rusinko, Jr. and E. Raats, *J. Phys. Chem.*, **59**, 245 (1955).
12. A. Zukal, M. M. Dubinin, O. Kadlec, T. G. Plachenov and R. Poolak, *Zhur. Fiz. Khim.*, **39**, 1198 (1965).
13. L. G. Joyner, E. P. Barret and R. Skold, *J. Am. Chem. Soc.*, **73**, 3155 (1951).
14. C. N. Cochran and L. A. Cosgrove, *J. Phys. Chem.*, **61**, 1417 (1957).
15. A. Guyer Jr., B. Bohlen and A. Guyer, *Helv. Chim. Acta.*, **42**, 2103 (1959).
16. H. L. Ritter and L. C. Erich, *Anal. Chem.*, **20**, 655 (1948).